A Lagrangian finite element method for non- Newtonian free-surface fluid flows and fluid-structure interaction problems

Massimiliano Cremonesi, Attilio Frangi, Umberto Perego

CSMA 2011
10e Colloque National en Calcul des Structures
9-13 Mai 2011, Presqu'île de Giens (Var)

A Lagrangian finite element method for non-Newtonian free-surface fluid flows and fluid-structure interaction problems

M. Cremonesi[1], F. Frangi[2], U. Perego[3]

[1] *Laboratoire de Mécanique et Technologie, École Normale Supérieure de Cachan, France, cremonesi@lmt.ens-cachan.fr*
[2] *Department of Structural Engineering, Politecnico di Milano, Italy, attilio.frangi@polimi.it*
[3] *Department od Structural Engineering, Politecnico di Milano, Italy, umberto.perego@polimi.it*

Résumé —
A Lagrangian Finite Element method is applied to the discretization of the Navier-Stokes equations to simulate fluid problems with significant evolution of the free-surfaces. The same approach is also used to treat fluid-structure interaction problems. Both Newtonian and non-Newtonian fluid behaviours are considered. Different examples are performed to show the potentialities of the approach.
Mots clés — Lagrangian fluid, free-surface, fluid-structure interaction, non-Newtonian fluids.

1 Introduction

A critical point in the simulation of the fluid flow problems is the treatment of the free surface. Similarly, in fluid-structure interaction problems the efficent determination of interface between solid and fluid, is always crucial. The Arbitrary Lagrangian Eulerian method (ALE), in which the movement of the fluid particles is independent of that of the mesh nodes, is often used to solve this kind of problems. Other possible solution schemes are based on the volume of fluid or level set algorithms. Meshfree and meshless methods are often used for their ability to recover the free-surfaces and the interfaces. In this work an other possibility to overcome the difficulties concerning the tracking of the interfaces is presented. A Lagrangian approach is used to describe both the fluid and the structural phases. In particular, a staggered scheme is considered in which the fluid is treated using a new implementation [1] of the Particle Finite Element Method (PFEM), first proposed by Oñate, Idelsohn and coworkes [2, 3], and the structure using a classical finite element method.

Using a Lagrangian approach for the fluid flow the convective terms in the momentum conservation equation, typical difficulty of the Eulerian framework, disappear. The difficulty is however transferred to the necessity of a frequent remeshing of the fluid domain. In fact, in a Lagrangian framework the position of element nodes is updated as a consequence of the fluid flow and the element distortion can become excessive. To avoid these distortions, a possible remedy consists of a systematic remeshing of the volume of the problem. To this purpose, an efficient Delaunay triangulation has been adopted. Moreover, to define the integration domain and to correctly impose the boundary conditions, an "alpha shape method" [4] is used.

The proposed Lagrangian Finite Element Method is particularly suited also for the solution of fluid-structure interaction problems in the presence of free-surfaces, in conjunction with a classical finite element method for the solid part.

2 Governing equations

The Particle Finite Element Method (PFEM) [2, 3] is conceived for the solution of fluid-dynamics problems using a Lagrangian approach based on the formulation of the Navier-Stokes equations in material coordinates. In the Lagrangian framework the equations of motion of a fluid can be written as :

$$\rho_0 \frac{D\mathbf{u}}{Dt} = \mathrm{Div}\Pi + \rho_0 \mathbf{b} \quad \text{in } \Omega_0 \times (0,T) \tag{1}$$

$$\mathrm{Div}\left(J\mathbf{F}^{-1}\mathbf{u}\right) = 0 \qquad \text{in } \Omega_0 \times (0,T) \tag{2}$$

where ρ_0 is the density of the fluid, $\mathbf{u}$ is the velocity, $\Pi = J\sigma\mathbf{F}^{-T}$ is the first Piola-Kirchhoff stress tensor, σ is the Cauchy stress tensor, $\mathbf{F}$ is the deformation gradient, J is the determinant of $\mathbf{F}$ and Ω_0 represents the initial (and reference) configuration. The Cauchy stress tensor σ can be related to the velocity $\mathbf{u}$ and to the pressure p by the relation :

$$\sigma = -p\mathbf{I} + \tau(\mathbf{u}) \tag{3}$$

where $\tau(\mathbf{u})$ represents the deviatoric stress. If a Newtonian constitutive law is considered, the deviatoric stress can be directly expressed as a function of the velocity :

$$\tau = \mu\left(\text{grad}\mathbf{u} + \text{grad}\mathbf{u}^T\right) \tag{4}$$

where μ is the viscosity of the fluid. If, insted, a non-Newtonian behaviour is considered, the deviatoric stress is a generic nonlinear function of the velocity.

2.1 Space discretization

To discretize in space the problem (1)-(2) an isoparametric finite element discretization is introduced. As explained in the next section, the same order of interpolation is used for both velocity and pressure unknows. The semi-discretized form of the equations (1)-(2) reads :

$$\mathbf{M}(\mathbf{x})\frac{D\mathbf{U}}{Dt} + \mathbf{K}(\mathbf{x})\mathbf{V} + \mathbf{D}^T(\mathbf{x})\mathbf{P} = \mathbf{B} \tag{5}$$

$$\mathbf{D}(\mathbf{x})\mathbf{U} = \mathbf{0} \tag{6}$$

where $\mathbf{M}$ is the mass matrix, $\mathbf{K}$ is the fluid stiffness matrix, $\mathbf{D}$ is the discretization of the divergence operator and $\mathbf{B}$ is the vector of external forces :

$$\begin{aligned}
M_{ab} &= \int_{\Omega_0} \rho_0 N_a N_b \mathbf{I} d\Omega_0 \\
D_{ab} &= \int_{\Omega_0} J N_a \text{Grad}(N_b)\mathbf{F}^{-1} d\Omega_0 \\
K_{ab} &= \int_{\Omega_0} \mu J \left(\text{Grad}(N_a)\mathbf{F}^{-1}\right) \otimes \left(\text{Grad}(N_b)\mathbf{F}^{-1}\right) d\Omega_0 \\
B_a &= \int_{\Omega_0} \rho_0 \mathbf{b} N_a \, d\,\Omega_0
\end{aligned}$$

where $\mathbf{I}$ is the identity matrix and N_a the nodal shape function. The matrix operators $\mathbf{K}$ and $\mathbf{D}$ clearly depend on the current configuration through the deformation gradient $\mathbf{F}$.

2.2 Pressure stabilization

In the present approach every time the mesh is regenerated (connecting the points with the Delauany triangulation), the informations related to the element are lost. The same occurs for informations related to nodes not coinciding with triangle vertices. Consequently, to avoid convecting data from the old to the new mesh, only vertx node data can be stored, and only linear shape functions can be used in the space discretization of the problem (1)-(2). To avoid spurious oscillations due to the fact that the *inf-sup condition* is not satisfied [5], a stabilization must be introduced. In particular a *pressure-stabilizing/Petrov-Galerkin* (PSPG) stabilization is adopted [6]. Introducing the stabilization in the finite element space discretization previously considered, the semi-discrete stabilized equations read :

$$\mathbf{M}(\mathbf{x})\frac{D\mathbf{U}}{Dt} + \mathbf{K}(\mathbf{x})\mathbf{V} + \mathbf{D}^T(\mathbf{x})\mathbf{P} = \mathbf{B} \tag{7}$$

$$\mathbf{C}(\mathbf{x})\frac{D\mathbf{U}}{Dt} + \mathbf{D}(\mathbf{x})\mathbf{V} + \mathbf{L}(\mathbf{x})\mathbf{P} = \mathbf{H}(\mathbf{x}) \tag{8}$$

where the matrices **C**, **L** and **H** are given by :

$$C_{ab} = \sum_{e=1}^{N_{el}} \int_{\Omega_0^e} \tau_{pspg}^e \text{Grad}(N_a) N_b d\Omega_0$$

$$L_{ab} = \sum_{e=1}^{N_{el}} \int_{\Omega_0^e} \frac{\tau_{pspg}^e}{\rho} \text{Grad}(N_a) \cdot \text{Grad}(N_b) \mathbf{F}^{-1} d\Omega_0$$

$$H_a = \sum_{e=1}^{N_{el}} \int_{\Omega_0^e} \tau_{pspg}^e \text{Grad}(N_a) \cdot \mathbf{b} d\Omega_0$$

and the stabilization parameter is defined as :

$$\tau_{pspg}^e = \frac{z_e}{2\|\mathbf{u}\|} \tag{9}$$

and z_e is the "element length" defined to be equal to the diameter of the circle which is area-equivalent to the element e.

2.3 Time integration

The time integration is performed with a classical backward Euler scheme. Introducing a partition of the time domain into N time steps of the same length Δt, and choosing as the reference configuration at time t^n, the discretized system reads :

$$\frac{1}{\Delta t}\mathbf{M}\left[\mathbf{U}^{n+1} - \mathbf{U}^n\right] + \mathbf{K}(\mathbf{U}^{n+1})\mathbf{U}^{n+1} + \mathbf{D}^T(\mathbf{U}^{n+1})\mathbf{P}^{n+1} = \mathbf{B} \tag{10}$$

$$\frac{1}{\Delta t}\mathbf{C}\left[\mathbf{U}^{n+1} - \mathbf{U}^n\right] + \mathbf{D}(\mathbf{U}^{n+1})\mathbf{U}^{n+1} + \mathbf{L}(\mathbf{U}^{n+1})\mathbf{P}^{n+1} = \mathbf{H} \tag{11}$$

where the matrices **K**, **D** and **L** and the vector **H** depend nonlinearly on the vector $\mathbf{U}^{n+1}$.

3 Description of the method

The PFEM, in the form implemented in the present work, consists of the following conceptual steps (see also [2] and reference therein). Figure 1 shows a pictorial representation of the steps.

1. Fill the fluid domain with a set of points referred to as "particles" (Figure 1(a)). The accuracy of the numerical solution is clearly dependent on the considered number of particles.
2. Generate a finite element mesh using the particles as nodes. This is achieved using a Delaunay triangulation (Figure 1(b)).
3. Identify the external and internal boundaries to compute the domain integrals and to impose correctly the boundary conditions (Figure 1(c)).
4. Solve the non-linear Lagrangian equations of motion (10)-(11) finding velocity and pressure at every node of the mesh.
5. Update the particle positions using the computed values of velocity and pressure (Figure 1(d)).
6. Check the mesh distortion :
   - if the mesh is too distorted go back to step 2 and repeat for the next time step.
   - if the mesh is not too distorted go back to step 3 and repeat for the next time step.

3.1 Mesh generation and identification of external boundaries

To solve the Lagrangian Navier-Stokes equations in a domain defined by the particles, a finite element mesh is necessary. A possibility to generate a mesh starting from a particle distribution is the Delaunay triangulation. The Delaunay triangulation generates the convex hull of the set of particles, i.e. the convex figure with minimum area that encloses all the particles belonging to the set.

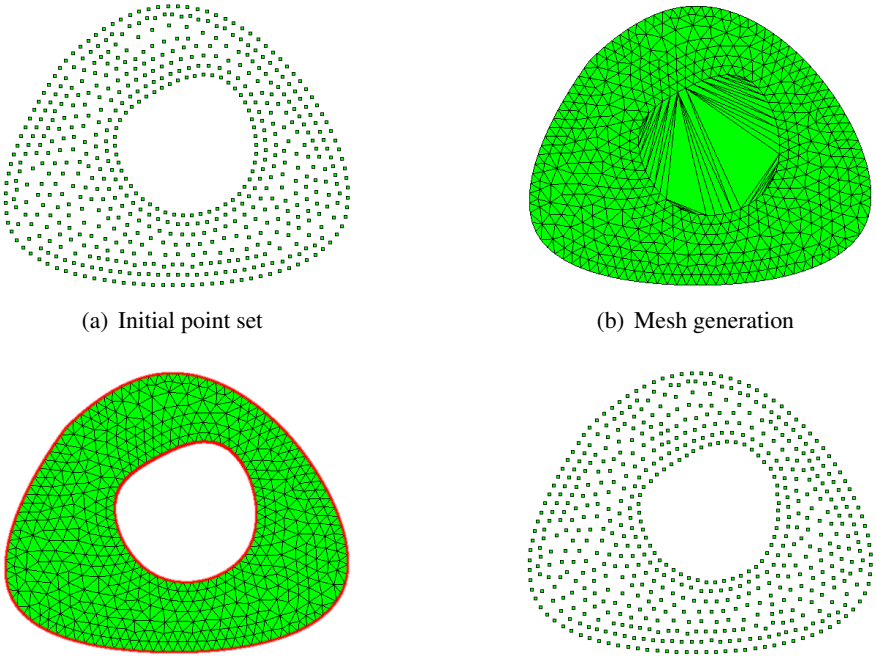

(a) Initial point set (b) Mesh generation

(c) Boundary identification (d) Update of the particle position

FIGURE 1 – Steps of Particle Finite Element Method

Therefore, in a Lagrangian framework the external boundary $\Gamma_t = \partial\Omega_t$ and the current volume Ω_t are defined by the position of the material particles. Every time that the mesh is regenerated with the Delaunay triangulation, the particles belonging to the boundary may change and the new boundary nodes (and therefore the particles) have to be identified. The identification process is divided in two phases :

– identification of the real shape of the particle distribution ;
– identification of the nodes that belong to the boundary.

The second phase is almost trivial, but the first one is critical. As introduced, the Delaunay triangulation generates the convex hull of the set of particles. However, the convex hull may be not conformal with the external boundaries. To clarify this problem, a set of points is shown in Figure 2(a) and its Delaunay triangulation in Figure 2(b). It is clear that the Delaunay triangulation does not match the real boundaries.

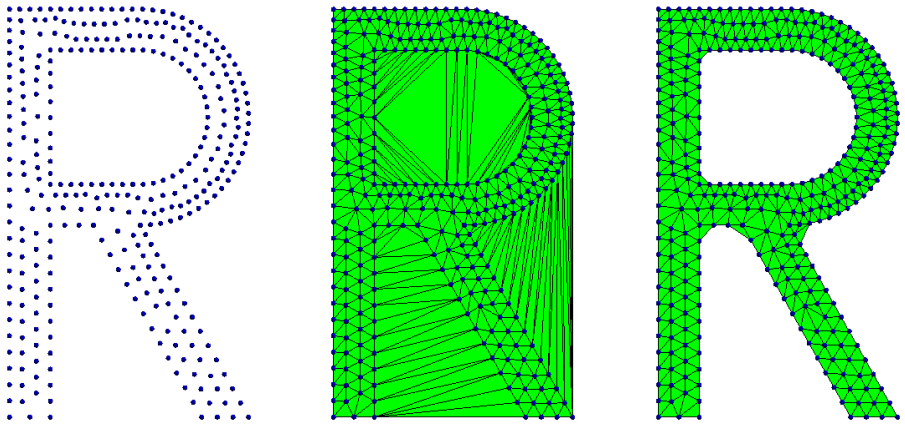

(a) (b) (c)

FIGURE 2 – (a) Distrubution of points, (b) Delaunay triangulation, (c) Delaunay triangulation with α-shape.

A possibility to overcome this problem is to correct the generated mesh using the so called α-shape method [4] as proposed in [7]. The key idea is to remove the unnecessary triangles from the mesh using a

criterion based on the mesh distortion. For each triangle e of the mesh, the minimal distance h_e between two nodes in the element and the radius R_e of the circumcircle of the element are defined. If h is computed as the mean value of all the h_e, the shape factor :

$$\alpha_e = \frac{R_e}{h} \geq \frac{1}{\sqrt{3}}, \tag{12}$$

is an index of the element distortion. It is worth recalling that $R_e/h_e = 1/\sqrt{3}$ is the ratio for an equilateral triangle. All the elements that do not satisfy the condition :

$$\alpha_e \leq \bar{\alpha} \tag{13}$$

are removed from the mesh, where $\bar{\alpha} \geq 1$ is assumed. Figure 2(c) shows the Delaunay triangulation coupled with the alpha-shape scheme for the example introduced before.

In general, increasing the value of $\bar{\alpha}$, fewer triangles are removed from the original mesh and, for $\bar{\alpha} \to \infty$, the original Delaunay triangulation is always recovered.

Once the unnecessary triangles are removed from the Delaunay triangulation, the particles which actually belong to the boundary can be identified.

The α-shape method can also be used for the identification of the fluid particles which separates from the rest of the domain. When a particle on the boundary is a vertex of only one triangle and the triangle is overly distorted, the particle is separated from the domain and all the mass of the triangle is assigned to this particle in order to preserve the total fluid mass. After separation, the motion of these particles is governed by the body force and the initial velocity which they are subjected to. At each new Delaunay triangulation, the separated particles become vertices of triangles. In the case that a separated particle has approached enough the fluid free boundary, the triangle is not eliminated by the α-shape method check and the particle is again incorporated in the fluid mass.

4 Fluid-structure interaction

The proposed Lagrangian Finite Element Method is particularly suited for the solution of fluid-structure interaction problems in the presence of free-surfaces, in conjunction with a classical finite element method for the solid part. A critical issue of fluid-structure interaction schemes is the identification of the contact interfaces between the solid and fluid domains. The evolution of the interaction surfaces is tracked using a novel algorithm which exploits the features of the Lagrangian approach based on the continuous remeshing introduced for the fluid solution. The proposed algorithm is based on the superposition of a set of fictitious fluid particles (called “ghost particles”) to the nodes of the solid domain, which can come in contact with the fluid domain. When the Delaunay triangulation is performed, the alpha-shape criterion selects those parts of the interface where the fluid particles can possibly come into contact with the structure. If the two discretized domains are not in contact, the fluid and the solid analyses are performed separately without any interaction. If instead parts of the two discretized domains are in contact, a coupled analysis is performed with a Dirichlet-Neumann iterative approach. The fundamental steps of the interaction can be listed as follows.

- Superpose a set of ghost particles to the solid surfaces which can possibly come into contact with the fluid domain.
- Perform the Delaunay triangulation.
- Apply the α-shape method to remove the unnecessary triangles.
- Check whether the fluid is in contact with the solid part. The fluid element is assumed to be in contact with the solid if at least one of its nodes is a ghost particle.
  - If the two discretized domains are not in contact, the fluid and the solid analyses are performed separately without any interaction.
  - If the two discretized domains are in contact, a coupled analysis is necessary.

5 Applications

The proposed scheme has been applied to both Newtonian and non-Newtonian fluids. Comparisons with numerical benchmarks and with experimental results are presented to show its potentialities.

5.1 Fluid-structure interaction : filling of a deformable container

The present approach has been used to simulate an example of a fluid-structure interaction problem involving large fluid motions with large displacements of the structure. Under the action of the gravity force a fluid drops down from a funnel-shaped rigid container into a thin elastic container. The elastic properties of the container are given as : Young modulus $E = 210\,\text{KPa}$, Poisson ratio $\nu = 0.3$ and density $\rho_s = 2000\,\text{Kg/m}^3$. For the fluid a fluid viscosity $\mu = 0.001\,\text{Kg/ms}$ and a density $\rho_f = 1000\,\text{Kg/m}^3$ are adopted. In the solution an initial fluid mesh of 5749 nodes and 11103 elements and a solid mesh of 2188 nodes and 3365 quadrilateral plane strain elements are adopted and a time step of 0.001 s is used. Figure 3 shows the deformation of the elastic container at different time step.

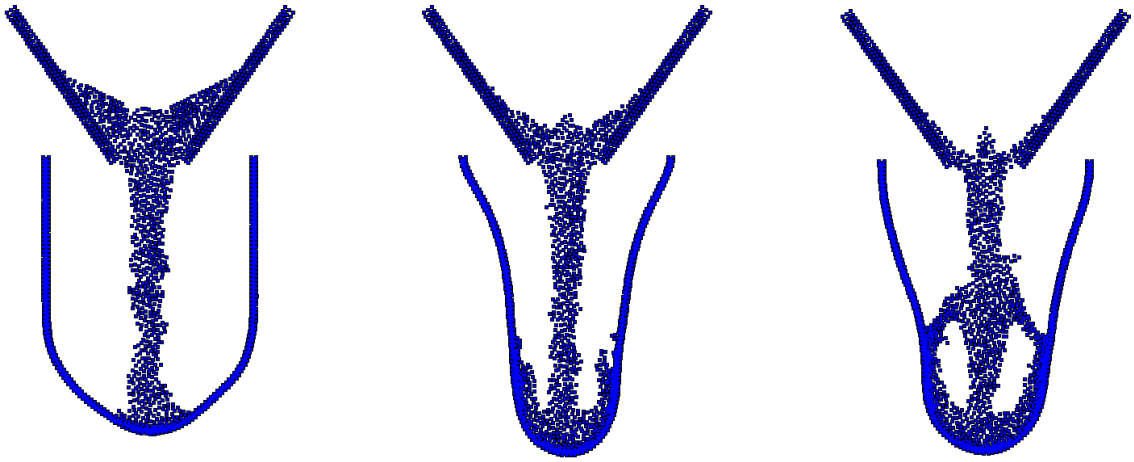

FIGURE 3 – Deformation of an elastic container. Snapshots at different time step.

5.2 Non-Newtonian fluids : slump flow test

The non-Newtonian solver has been used to simulate typical tests on fresh concrete, mortar and cement pastes. In general, yield stress and viscosity are parameters used to characterize the workability of this kind of materials. The experimental determination of these parameters is a research topic of recent years. However, in the identification of parameters an efficient numerical tool can be also very useful. To this purpose, the non-Newtonian solver is used to simulate typical tests widely used in the experimental identification of the rheological properties of fresh cement paste and concrete. For the cement pastes and mortars a Bingham constitutive behaviour, which is the simplest model encompassing the concept of yield stress, is considered. Using the Papanastasiou approximation [8], the Bingham behaviour can be described as a relationship between deviatoric stress and velocity :

$$\tau = \tilde{\mu}\,\varepsilon(\mathbf{u}) \tag{14}$$

$$\tilde{\mu} = \mu + \frac{\tau_0}{\|\varepsilon\|}\left(1 - e^{-n\|\varepsilon\|}\right) \tag{15}$$

where $\varepsilon(\mathbf{u}) = \left(\text{grad}\mathbf{u} + \text{grad}\mathbf{u}^T\right)$ is the symmetric part of the gradient of the velocity.

Figure 4 shows the simulation of a typical slump flow test. A rigid cone, open at both ends, is filled in with fresh cement paste or concrete, then the cone is suddenly raised allowing the fluid concrete to flow onto a board. The material will move only if the yield stress is exceeded and will stop when the stress is below the yield stress. Table 1 shows a comparison between the experimental radius and the radius computed with the present approach for different values of density, viscosity and yield stress for cement pastes. A good agreement can be observed between experimental and numerical results. Details about the numerical simulation of these tests can be found in [9].

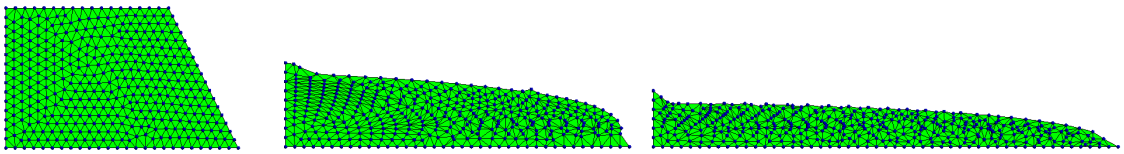

FIGURE 4 – Mini-slump-flow test. Snapshots at different time steps for a cement paste.

density (Kg/m^3)	viscosity (Pa s)	yield stress (Pa)	exp. radius (m)	computed radius (m)
2252	4.018	18.0182	0.2249	0.2200
2242	3.511	7.4457	0.2668	0.2520
2231	3.009	2.4997	0.3333	0.3226
2252	5.014	25.8860	0.2249	0.2228
2242	3.836	10.6969	0.2682	0.2804
2231	3.585	3.5913	0.3333	0.3291

TABLE 1 – Mini-slump-flow test : comparisons for varying density, viscosity and yield stress for cement pastes.

5.3 Deformable landslide simulation

The proposed approach is then used to simulate the wave generated by a deformable mass of granular material sliding in a water channel. This example is particularly interesting because impulse waves in bays, lakes or reservoirs generated by landslides or rock falls may propagate with possibly catastrophic consequences for the surronding enviroment.

For the numerical simulation of the sliding mass a non-Newtonian Bingham fluid behaviour is assumed, while a classical Newtonian behaviour is considered for the water [10]. Figure 5 shows snapshots of the analysis at different time steps.

Références

[1] M. Cremonesi, A. Frangi, and U. Perego. A lagrangian finite element approach for the analysis of fuid-structure interaction problems. *International Journal for Numerical Methods in Engineering*, (doi :10.1002/nme.2911), 2010.

[2] E. Oñate, S.R. Idelsohn, F. Del Pin, and R. Aubry. The particle finite element method. An overview. *International Journal of Computational Methods*, 1(2) :267–307, 2004.

[3] S.R. Idelsohn, E. Oñate, and F. Del Pin. The particle finite element method : a powerful tool to solve incompressible flows with free-surfaces and breaking waves. *International Journal for Numerical Methods in Engineering*, 61(7) :964–989, 2004.

[4] H. Edelsbrunner and E. P. Mucke. Three dimensional alpha shapes. *ACM Transactions on Graphics*, 13(1) :43–72, January 1994.

[5] F. Brezzi and M. Fortin. *Mixed and Hybrid Finite Element Method*. Springer-Veralg, 1991.

[6] T. E. Tezduyar, S. Mittal, S. E. Ray, and R. Shih. Incompressible flow computations with stabilized bilinear and linear equal-order-interpolation velocity-pressure elements. *Computer Methods in Applied Mechanics and Engineering*, 95(2) :221–242, March 1992.

[7] S. R. Idelsohn, E. Oñate, and F. Del Pin. A lagrangian meshless finite element method applied to fluid-structure interaction problems. *Computers & Structures*, 81(8-11) :655–671, May 2003.

[8] T. C. Papanastasiou. Flows of materials with yield. *Journal of Rheology*, 31(5) :385–404, 1987.

[9] M. Cremonesi, L. Ferrara, A. Frangi, and U. Perego. Simulation of the flow of fresh cementitious suspensions by a lagrangian finite element approach,. *Journal of Non-Newtonian Fluid Mechanics*, 165 :1555–1563, 2010.

[10] M. Cremonesi, A. Frangi, and U. Perego. A lagrangian finite element approach for the simulation of water-waves induced by landslides,. *Computers and Structures*, doi :10.1016/j.compstruc.2010.12.005, 2011.

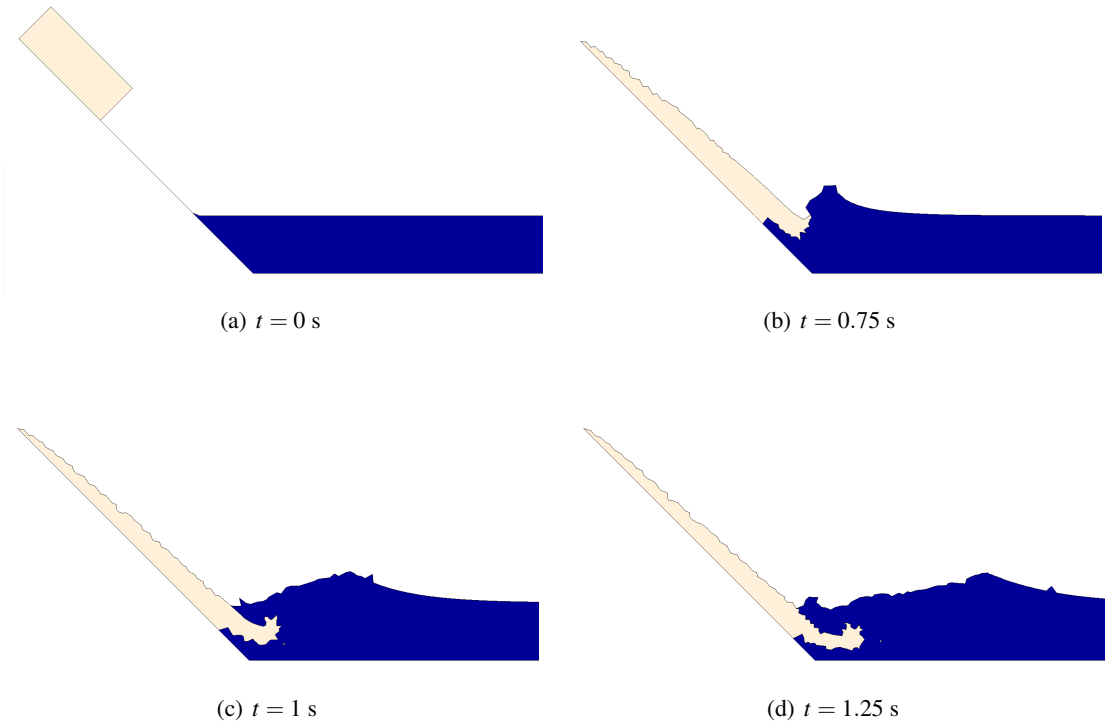

(a) $t = 0$ s (b) $t = 0.75$ s

(c) $t = 1$ s (d) $t = 1.25$ s

FIGURE 5 – Landslide without initial velocity. Snapshots at different time steps.